Scientific Research Publishing

Open Journal of Geology, 2025, 15(12), 1009-1028
https://www.scirp.org/journal/ojg
ISSN Online: 2161-7589
ISSN Print: 2161-7570

New Geological Data on the Inselbergs of Anié, Togo (West Africa)

Sarakawa Abalo Malibida Kpanzou[1,2*], Gnanwasou Alayi[1], Koffi Evenyon Kassegne[1], Yaovi Edem Baite[2], Ouro-Djobo Essoavana Samah[2], Mahaman Sani Tairou[1], Yao Agbossoumondé[1]

[1]Département de Géologie, Faculté des sciences, Université de Lomé, Lomé, Togo
[2]Département de Génie Civil, Centre Régional de Formation pour Entretien Routier (CERFER), Lomé, Togo
Email: *germalibida@gmail.com

How to cite this paper: Kpanzou, S.A.M., Alayi, G., Kassegne, K.E., Baite, Y.E., Samah, O.-D.E., Tairou, M.S. and Agbossoumondé, Y. (2025) New Geological Data on the Inselbergs of Anié, Togo (West Africa). *Open Journal of Geology*, **15**, 1009-1028.
https://doi.org/10.4236/ojg.2025.1512053

Received: November 21, 2025
Accepted: December 20, 2025
Published: December 23, 2025

Abstract

The Anié unit, located in central Togo, belongs to the suture zone of the Pan-African Dahomeyide belt. The aim of this work is to contribute to the updating of geological data focused on the lithostructural organization, petrography, and geochemistry of the rocks in this unit. The methodology used is based on a synthesis of previous work, geological mapping coupled with structural analysis, a petrographic study of thin sections, and a geochemical study using geotectonic discrimination diagrams. The results obtained show that the Anié unit is composed of granulites tectonically encased in gneisses. These granulites have a mineralogy of plagioclase, clinopyroxene, amphibole, biotite, and quartz. This paragenesis reflects a metamorphic evolution from granulitization to retromorphosis in the amphibolite facies. Geochemical data show that the rocks of the Anié unit are metaluminous. They have a calc-alkaline affinity and are more enriched in LREE than in HREE. Negative anomalies in Nb-Ta and Zr indicate magma from subduction zones. These rocks derive from an OIB (oceanic island basalts) type mantle source, which was modified in a subduction context associated with the nappes emplacement.

Keywords

Geology, Inselbergs, Anié, Dahomeyide, Togo

1. Introduction

In the Pan-African Dahomeyide belt, the basic to ultrabasic complexes of Dérouvarou (Benin), Kabyè-Kpaza, Djabatouré-Anié, Agou-Ahito (Togo), and Shaï or Akuse (Ghana) form a submeridian mountainous belt that marks the suture zone

[1]-[5]. These complexes are considered to be highly metamorphosed metamagmatic assemblages composed of ultramafic rocks, gabbroic metacumulates, metagabbros, pyroxenites, amphibolites, and granulites [1]-[3] [6]-[10]. The Djabatouré-Anié complex, located in central Togo, is composed of small units of basic to ultrabasic rocks [10] [11]. Among the units that make up this complex is the Anié unit, located in the southeast of the complex and represented by small hills (inselbergs) oriented W-E. The work of [12] partially addressed the petrographic and structural characteristics of the inselbergs of the Anié unit. According to this work, the inselbergs of the Anié unit are composed mainly of metadiorites cut by pegmatite veins of highly variable directions. Within these inselbergs, tectono-metamorphic foliation is not very pronounced and varies in both direction and dip. Like the other units with which they form the Djabatouré-Anié complex, the lithostructural and geochemical characteristics remain undefined or poorly understood [10] [12]. This contribution is therefore part of the updating of geological data for the Anié unit in terms of lithostructure, petrography, and geochemistry.

2. Geological Setting

The Pan-African Dahomeyide belt [13] (**Figure 1**) is the result of a long process of convergence that led to the collision between the Benino-Nigerian shield and the southeastern margin of the West African craton at the end of the Neoproterozoic [14]-[17]. The southern segment of the trans-Saharan orogen comprises, in its frontal part, a submeridian belt of basic to ultrabasic massifs building the suture zone (**Figure 1**). This string of beads marks the boundary between the external zone to the west and the internal zone to the east.

The units of the external zone of the Dahomeyide are structured in stacks of layers and scales carried westward to the Volta Basin [15] [18] [19]. The external-most nappes consist of various metasediments (sandstone-quartzite, hematite, metasilexite, schist, metaconglomerate, and metadiamictite), which are the lateral and tectono-metamorphic equivalents of the lower and middle megasequences of the Volta Basin [20] [21]. These nappes form the structural units of Buem and Atacora (**Figure 1**) and tectonically support the nappes of the external orthogneiss units (Kara-Niamtougou unit; Kpalimé-Amlamé unit; Mô plain unit) [22] [23]. The latter are considered to be evidence of the Eburnean substratum (2000 ± 200 Ma), which was largely remobilized by Pan-African thermo-tectonics [24]-[28].

The massifs in the suture zone (the best known of which are those of Dérouvarou, Kabyè-Kpaza, Djabatouré-Anié, Agou-Ahito, and Shai or Akuse (**Figure 1**) are identified as assemblages of eclogitic to granulitic nappes overlapping the external units [9] [10] [19]. They consist of various granulites and sometimes eclogites, associated with metasediments (mica schists, quartzites, and garnet and kyanite bearing gneisses), fragments of pyroxenites and carbonatites, and retromorphic equivalents (amphibolites, talcschists, and serpentinites) [2] [29]. These massifs are evidence of the Dohomeyides subduction-collision

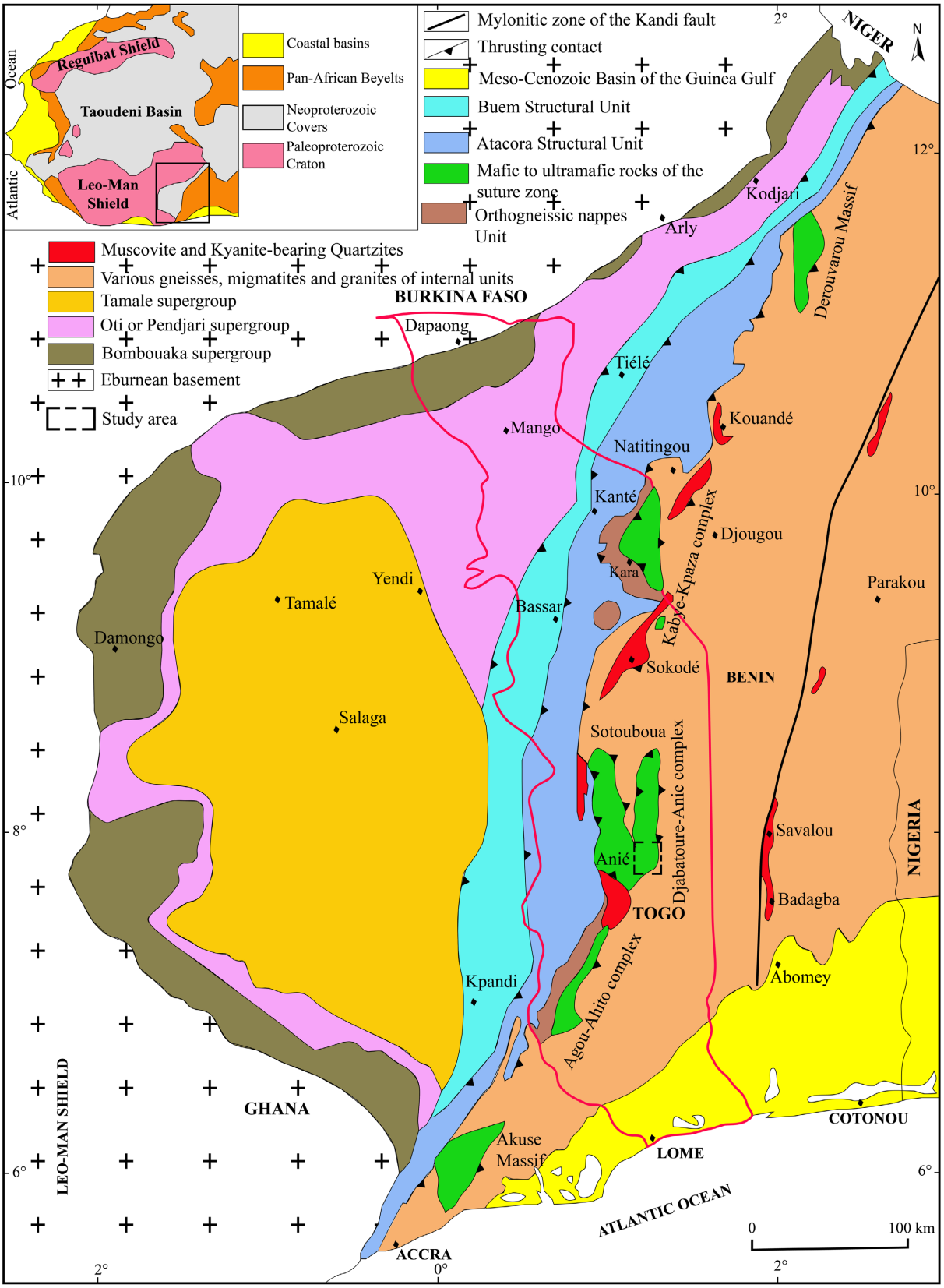

Figure 1. Simplified geological map showing the main structural domains of the Pan-African Dahomeyide belt and its foreland (from [13]; slightly modified) indicating the Anié unit.

process [4] [10] [26] [30]-[35].

The Dahomeyide internal zone corresponds to the southern portion of the trans-Saharan metacraton [36]. This is the area on which the vast Benino-Nigerian peneplain is established. Its western front is roughly delimited by the string of massifs in the suture zone (**Figure 1**). This portion of the metacraton consists of a gneisso-migmatitic basement complex, bearing metavolcanic-sedimentary belts and more or less invaded by granitoids of Pan-African age [11] [37]-[42].

3. Methodology

The methodological approach of our study consists of a literature review, followed by fieldwork, laboratory analyses, data processing and analysis. The literature review allowed us to summarize previous work on regional geology and the geology of the study area. The field campaign allowed us to search for outcrops, collect samples, describe these outcrops and samples in situ in macroscopic terms, take structural measurements, and survey geological cross-sections. Sampling was carried out on rocks in situ using a geologist's hammer. We georeferenced the outcrops and sample collection stations using a Garmin eTrex Legend H GPS device. A total of seventy (70) samples were collected, some of which were used to prepare twenty-five (25) thin sections for microscopic observation focused on microstructures and mineralogical compositions. The structural measurements collected were used to create rosettes using TectonicsFP software and to produce stereograms by projection onto a Wulff net (upper hemisphere). The summary geochemical study was based on chemical analysis data (major elements, trace elements, and rare earth elements) from five (05) carefully selected rock samples. These analyses were conducted at the scientific instrumentation center at the University of Granada (Spain). The analytical approach adopted is as follows:

1) Major elements oxides were determined with a Philips Magix Pro (Pw-2440) X-ray fluorescence (XRF) equipment after melting the rock sample in a solution with tetra lithium borate. The characteristic precision as determined from standards AN-G and BEN, was better than ±1.5% (relative error) for an analyte concentration of 10 wt.%. The iron content is expressed as FeO* total. The molar ratio MgO/(MgO+FeO*) is abbreviated Mg#. Zirconium was determined with the same instrument using the same glass beads with a precision better than ± 0.2% for 5 ppm Zr. Loss on Ignition (LOI) was determined by weight difference before and after ignition of samples in a furnace. In the diagrams, oxide concentrations are reported in an anhydrous (volatile free) basis.

2) Trace elements, except Zr, were determined by an Inductively Coupled Plasma-Mass Spectrometry (ICP-MS) after HNO_3 + HF digestion of 0.1000 g of sample powder in a Teflon-lined vessel at 180˚C and 200 psi for 30 min, evaporation to dryness and subsequent dissolution in 100 ml of 4 vol.% HNO_3; the precision, as determined from standards PMS, WSE, UBN, BEN, BR and AGV run as unknowns, was better than ± 2% for analyte concentrations of 50 ppm and ± 5% for analyte concentrations of 5 ppm.

The results of the chemical analyses are shown in Table 1. The location of the samples analyzed is shown in Figure 2. The field and chemical analysis data were compiled in Excel and imported into various software programs (GCDkit, QGIS, etc.) for specific processing. For the processing of geochemical data, we normalized the major elements to 100% on an anhydrous basis.

Table 1. Composition in major elements (wt%), trace elements (ppm), and rare earth elements (ppm) of the Anié unit rocks.

(a)

Sample	Granulites				
	2A	3A	6	9	20
Xcoord.	E1˚14'32.8"	E1˚14'38.4"	E1˚14'59.4"	E1˚17'41.4"	E1˚08'49.7"
Ycoord.	N7˚44'49.4"	N7˚44'47.3"	N7˚45'18.4"	N7˚47'36.7"	N7˚47'40.7"
SiO_2 (wt%)	55.68	58.84	54.99	53.8	55.84
Al_2O_3	17.86	16.66	17.34	18.65	18.24
Fe_2O_3	6.91	6.7	7.92	8.5	7.31
MnO	0.09	0.09	0.11	0.11	0.09
MgO	4.62	3.84	4.82	4.36	3.68
CaO	7.45	6.18	7.7	7.66	7.02
Na_2O	4.35	4.35	4.01	4.28	4.79
K_2O	0.9	1.27	1.00	0.85	0.99
TiO_2	1.09	1.03	1.00	0.96	1.21
P_2O_5	0.29	0.24	0.25	0.19	0.3
LOI	0.27	0.39	0.43	0.14	0.16
Total	**99.51**	**99.59**	**99.57**	**99.5**	**99.63**

(b)

Sample	Granulites				
	2A	3A	6	9	20
Rb (ppm)	15.28	20.42	19.9	5.26	7.97
Ba	300.97	400.21	303.64	607.51	365.86
Nb	3.29	4.43	3.57	3.64	4.63
Ta	0.26	0.36	0.28	0.22	0.31
Sr	797.41	646.27	567.13	822.76	672.29
Zr	106.1	161.7	128.9	73.2	145.9
Y	11.09	14.36	14.34	13.72	15.17
Hf	0.62	0.63	0.59	0.49	0.56
Ni	83.31	59.8	70.76	38.2	47.83

Continued

Cr	124.99	90.5	91.32	38.84	61.29
V	162.77	140.34	175.76	202.08	156.73
U	0.41	0.43	0.48	0.08	0.19
Th	1.22	1.02	1.4	0.00	0.00
Sc	15.15	13.9	18.65	15.76	14.91
Co	47.00	48.9	45.19	42.25	39.69
Cu	43.64	92.36	86.03	64.37	53.17
Zn	125.11	74.66	79.42	87.95	80.19
Mo	4.15	4.68	2.96	2.67	3.25
Cs	0.58	0.51	0.71	0.12	0.24
Li	11.25	8.5	10.43	8.22	4.94
Be	0.91	1.14	0.9	1.06	1.1
Ga	21.33	20.28	20.29	21.74	22.3
Sn	0.55	0.93	0.6	0.57	1.06
Tl	0.08	0.1	0.09	0.04	0.05
Pb	4.55	6.15	4.76	4.92	5.73
La	11.89	15.22	12.33	15.55	15.21
Ce	27.88	34.88	28.01	31.87	35.77
Pr	3.77	4.69	3.74	4.01	4.8
Nd	16.67	20.39	16.32	17.06	21.24
Sm	3.53	4.29	3.57	3.53	4.49
Eu	1.12	1.38	1.2	1.2	1.28
Gd	2.28	2.88	2.57	2.48	3.09
Tb	0.3	0.41	0.37	0.34	0.43
Dy	1.81	2.36	2.28	2.14	2.49
Ho	0.38	0.48	0.48	0.46	0.5
Er	1.00	1.23	1.26	1.23	1.29
Tm	0.15	0.18	0.19	0.19	0.19
Yb	0.9	1.09	1.13	1.13	1.11
Lu	0.13	0.16	0.17	0.17	0.16
Eu/Eu*	1.18	1.18	1.19	1.21	1.03
(La)N	30.96	39.64	32.11	40.49	36.61
(Sm)N	15.24	18.52	15.42	15.24	19.39
(Gd)N	7.44	9.40	8.38	8.09	10.08
(Yb)N	3.91	4.74	4.91	4.91	4.83

Continued

(La/Sm)N	2.03	2.14	2.08	2.66	2.04
(Gd/Yb)N	1.90	1.98	1.71	1.65	2.09
(La/Yb)N	7.91	8.36	6.54	8.24	8.21
ΣREE	71.81	89.64	73.62	81.36	92.05

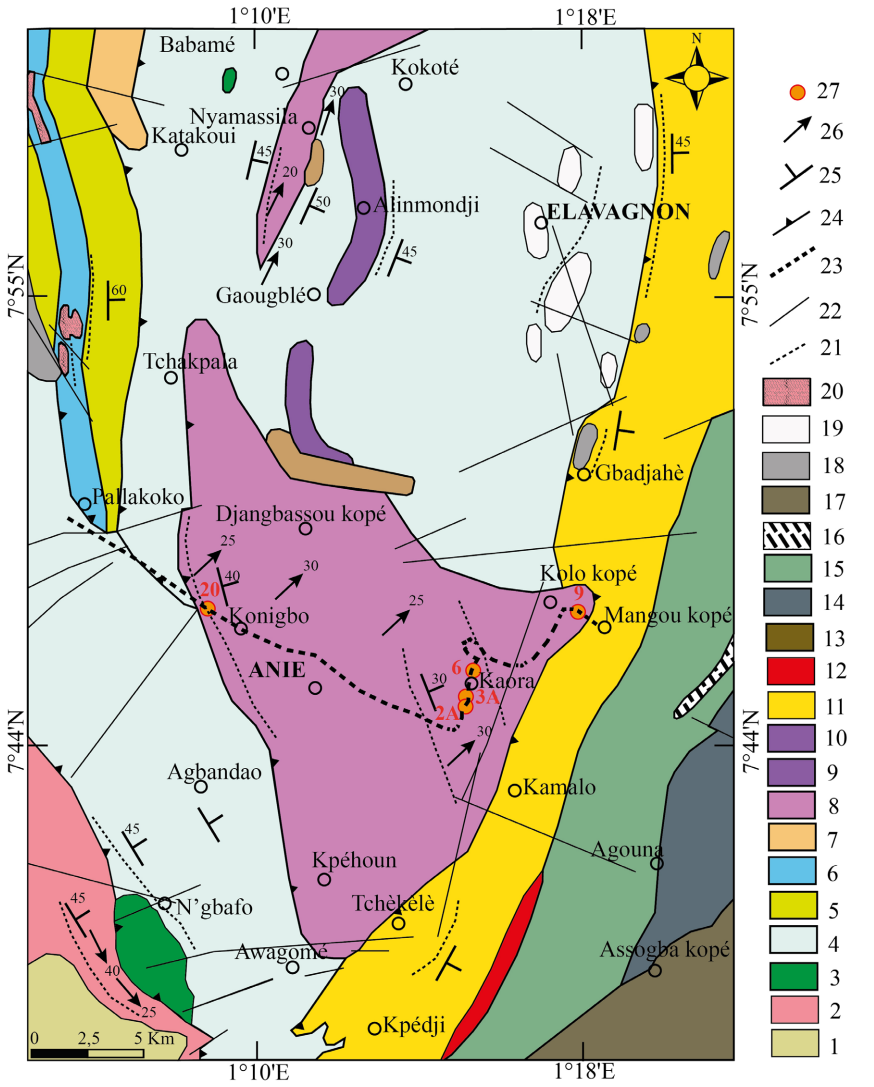

Figure 2. Schematic map of the Anié area (modified from the geological map by [12]). 1: sericite and muscovite bearing schists; 2: feldspathic quartzites; 3: serpentinites; 4: biotite and amphibole bearing gneisses; 5: 2-mica bearing paragneisses; 6: biotite bearing micaschists; 7: 2-mica bearing gneisses; 8: granulites; 9: biotite and amphibole bearing metatexites; 10: biotite and amphibole bearing orthogneiss; 11: two-mica and amphibole bearing gneiss; 12: fine biotite and amphibole bearing metagranites; 13: biotite and garnet bearing migmatitic gneiss; 14: biotite and muscovite bearing metatexites; 15: biotite bearing metatexites; 16: biotite and muscovite bearing leptynites; 17: pyroxenites; 18: amphibolites; 19: leptynitic gneisses; 20: biotite bearing quartzites; 21: traces of the main Sn+1 foliation; 22: faults; 23: cross-section itinerary; 24: overlapping contact; 25: orientation of Sn+1 planes; 26: Ln+1 lineations; 27: sampling points.

4. Results

4.1. Lithostructural Characteristics

The inselbergs of Anié unit (Figure 2) are mainly composed of granulites tectonically encased in gneisses (Figure 3).

The granulites outcrop in large hills (Figures 4(a)-(c)) in banks ranging from

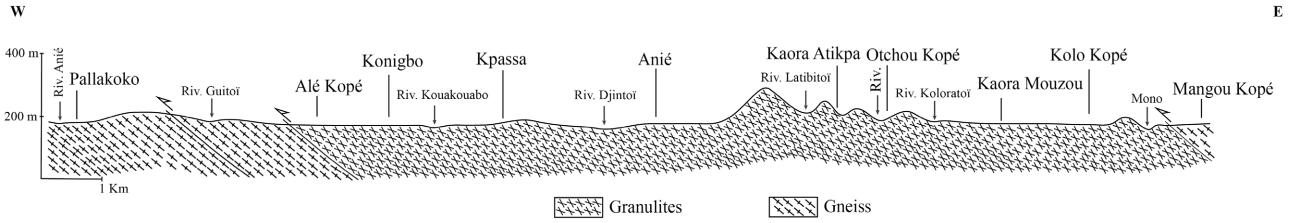

Figure 3. Synthetic cross-section showing the lithostructural organization of the Anié unit.

Figure 4. Petrostructural characteristics of granulites and gneisses from the Anié unit. (a)-(c): granulite inselbergs; (d) granulites showing ferromagnesian enclaves displaced by pegmatite veins in a anticlockwise direction, indicating a sinistral shear; (e) pegmatite veins; (f) prismatic amphibole in a pegmatite vein; (g) gneiss showing veins displaced clockwise, indicating a dextral shear; (h) gneiss showing displaced veins indicating both a dextral shear and a sinistral shear; (i) eyed gneiss showing blasts that have undergone clockwise rotation, indicating a dextral shear.

a few meters to tens of meters thick. They are grayish and shows a sometimes coarse foliation with medium to fine grains. They are cut by quartz-feldspar veins and veinlets displacing mesocratic enclaves expressing a sinistral shear (**Figure 4(d)** and **Figure 4(e)**). The main Sn + 1 (syn-shear planar foliation) foliation is oriented N140˚ to N160˚, with dips of 30˚ to 60˚ towards the east (**Figure 5(a)**). The biotite-molded plagioclase blasts (main Sn + 1 foliation) observed in thin sections (**Figure 6(a)** and **Figure 6(b)**) have undergone clockwise rotation, indicating dextral shearing. These blasts show Sn foliation that is oblique to the Sn + 1 foliation. The Sn + 1 planes carry mineral lineations of mica stretching Ln + 1 (mineral stretching line) dipping 25˚ to 60˚ towards the NE (**Figure 5(a)**). The fractures are oriented N-S and WNW-ESE (**Figure 5(b)**). The veins cutting these rocks are oriented NE-SW (**Figure 5(c)**).

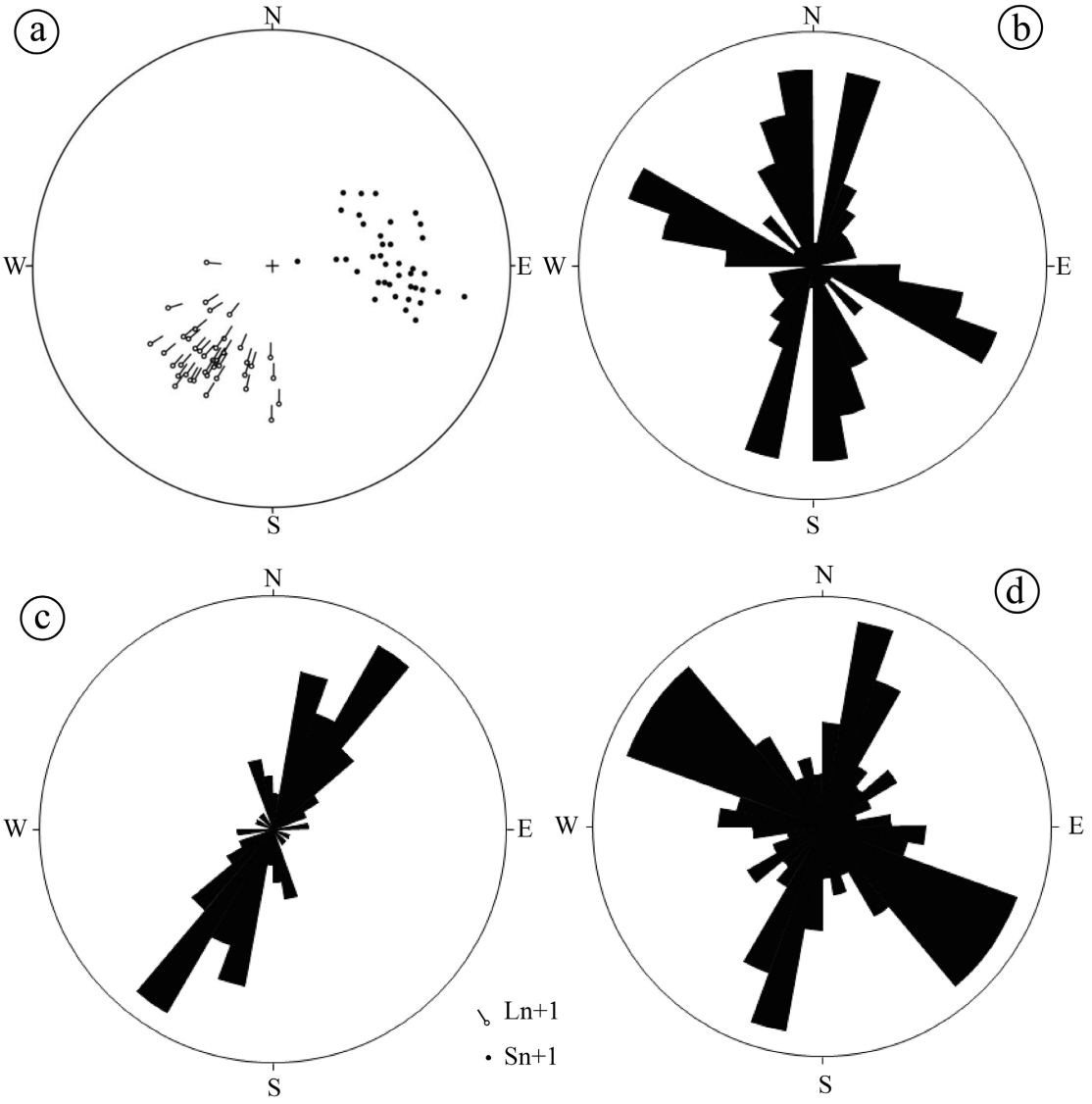

Figure 5. Stereogram (a) and synthetic rose-diagrams of structural elements identified on granulites (b and c) and hosted gneisses (d).

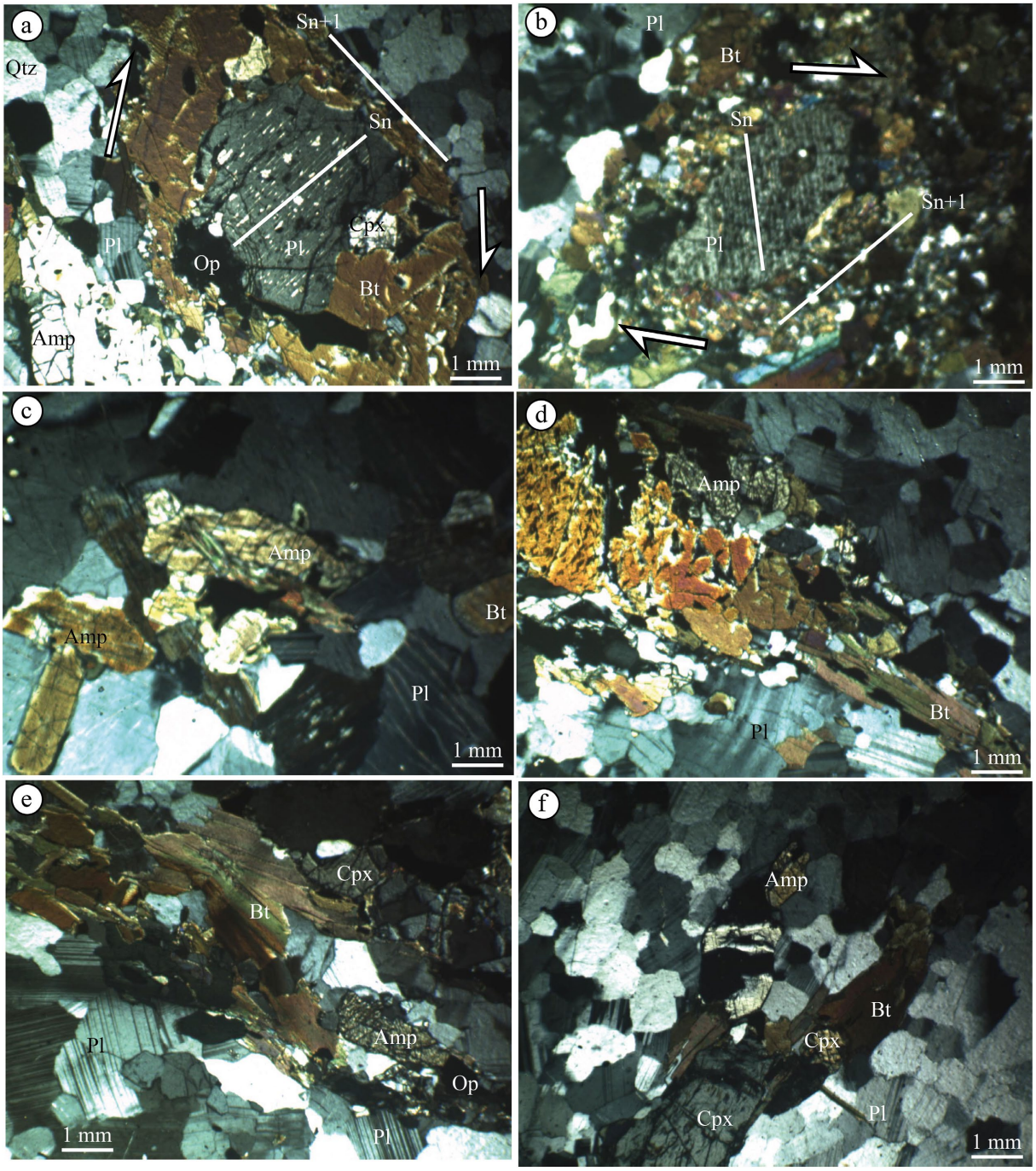

Figure 6. Some petrostructural aspects of the granulites of the Anié unit.

Gneisses outcrops at the contact with granulites. They are grayish, foliated and sometimes augen. The foliated gneisses are cut by quartz-feldspar veins that displace them clockwise, indicating a dextral shear, and anticlockwise, indicating a sinistral shear (**Figure 4(h)**). The eyed gneisses have blasts that have undergone clockwise rotation, indicating a dextral shear (**Figure 4(i)**). The main fracture directions are NW-SE and NNE-SSW (**Figure 5(d)**). In places, Sn + 2 (tectonic foliation or schistosity, formed after two previous deformations) crenulation schis-

tosity is observed, marked by the movement of the veins that have displaced the main Sn + 1 foliation in an anticlockwise direction, indicating a sinistral shear (**Figure 4(h)**).

4.2. Petrographic Characteristics

The granulites outcrop in banks ranging from one to several meters thick or in slabs (**Figures 4(a)-(c)**). They are grayish, with a foliated structure that is sometimes coarse, and medium to fine-grained (**Figure 4(g)**). They contain mesocratic basic enclaves and are cut by quartz-feldspar veins and veinlets containing prismatic amphiboles (**Figure 4(f)**). Microscopically, they have a granoblastic texture, sometimes granolepidoblastic with plagioclase (Pl), clinopyroxene (Cpx), amphibole (Hbl), biotite (Bt) and quartz (Qtz). Plagioclases are abundant and occur in aggregates, generally zoned with the presence of polysynthetic twins (**Figure 6**). The clinopyroxenes are intensely cracked and elongated in the main Sn + 1 foliation. They contain opaque minerals in their cracks and cleavages. Amphiboles are prismatic green phenocrystals, also elongated in the main Sn + 1 foliation. They are highly fractured and rich in opaque mineral and quartz inclusions. Biotite forms beds that constitute the main foliation and molds the plagioclase blasts (**Figure 6(a)** and **Figure 6(b)**). It appears as yellow to reddish-brown elongated phenocrystals lamellae. Quartz is quite rare.

The host gneisses are whitish to grayish, with a foliated structure, sometimes augen. They are generally cut by quartz-feldspar veins and veinlets. At the outcrop, they display a mineralogy of plagioclase, quartz, biotite, muscovite, and amphibole (**Figure 4(h)** and **Figure 4(i)**).

4.3. Geochemical Characteristics

4.3.1. Majors Elements Distribution

The rocks of the Anié unit are characterized by silica contents ranging between 53.80 and 58.84 wt% (**Table 1**). They show high values of Al_2O_3, reaching up to 18.65 wt%, and Sr, reaching up to 822.76 ppm. The MgO (3.68 to 4.84 wt%) and Fe_2O_3 (6.7 to 8.5 wt%) contents are low.

The major elements vs. SiO_2 diagram [43] (**Figure 7**) shows that the granulites of the Anié unit have a positive correlation between SiO_2 and K_2O, TiO_2, P_2O_5 and a negative correlation with Al_2O_3, FeOt, MgO, MnO, and CaO.

4.3.2. Traces and Rare Earth Elements Distribution

In the diagrams showing the variation of traces elements vs. SiO_2 [43] (**Figure 8**), the rocks of the Anié unit show a positive correlation between SiO_2 and Rb, La, Ni, Cr, Zr, Ce, Y, and a negative correlation with Ba and Sr.

The rare earth spectra normalized to the primitive mantle of [44] (**Figure 9(a)**) and [45] (**Figure 9(b)**) show that the rocks of the Anié unit are highly fractionated ($6.54 \leq (La/Yb)N \leq 8.36$). These rocks are more enriched in light rare earth elements ($2.03 \leq (La/Sm)N \leq 2.66$) than in heavy rare earth elements ($1.65 \leq (Gd/Yb)N \leq 2.09$), whose spectra are almost flat. They show negative anomalies in Nb-Ta, Ce,

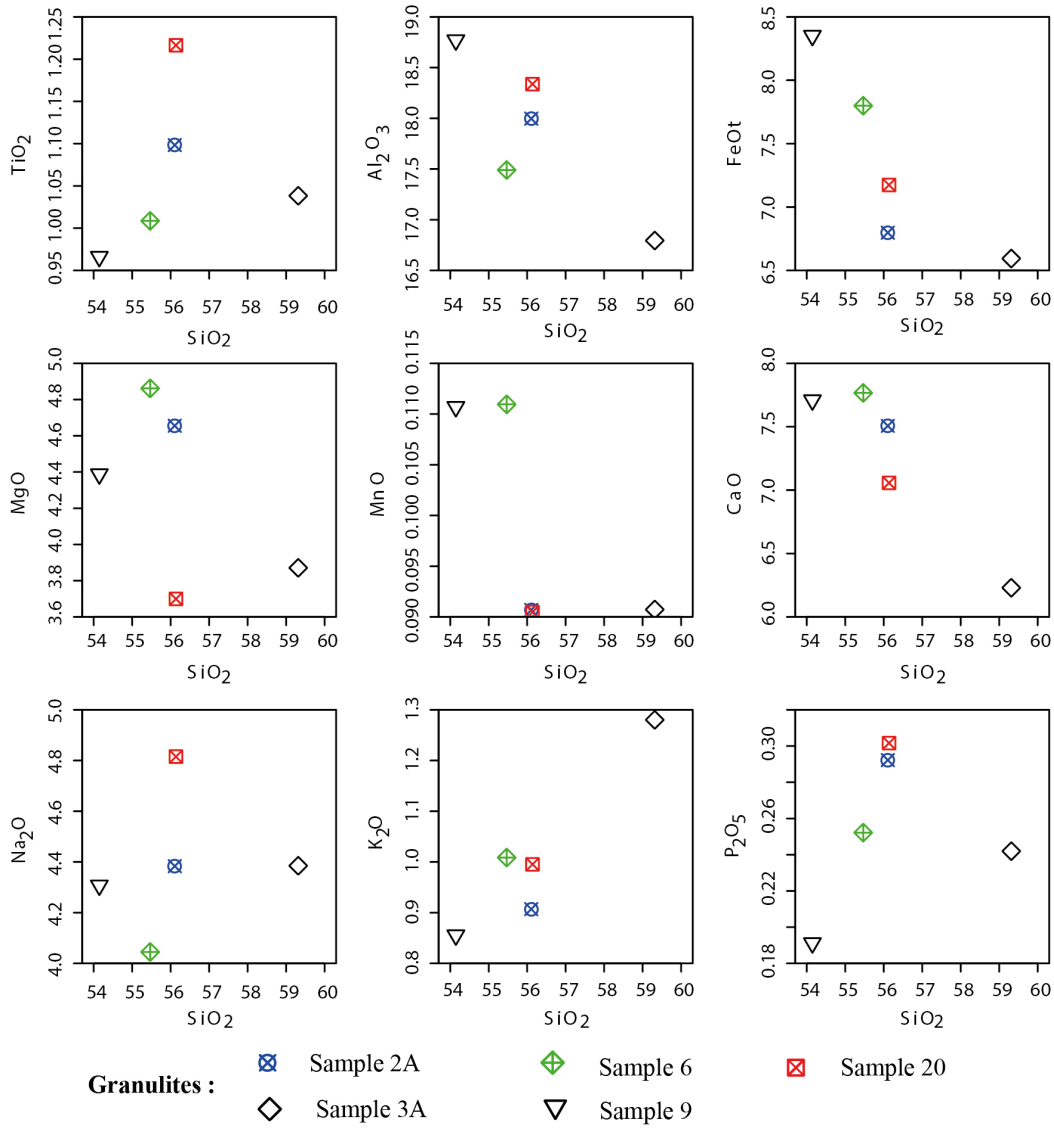

Figure 7. Diagram of major elements vs. SiO_2 [43] in rocks from the Anié unit.

Pr, Zr and positive anomalies in Ba, U, La, Pb, Sr, Sm.

4.3.3. Type of Rocks and Geodynamic Context

The rocks of the Anié unit appear in the diagram by [46] in the diorite field (**Figure 10(a)**). The diagrams by [47] (**Figure 10(b)**) and [48] (**Figure 10(c)**) indicate that the rocks of this unit have a calc-alkaline affinity. The diagram by [49] shows that these rocks are metaluminous (**Figure 10(d)**). The diagram by [50] shows that the rocks of the Anié unit belong to the orogenic domain (**Figure 10(e)**). [51] classifies them in the oceanic island basalt (OIB) field (**Figure 10(f)**).

5. Synthesis and Discussions

In terms of lithostructure, the granulites of the Anié inselbergs mostly correspond to large hills, sometimes with metric to decametric benches or slabs intersected

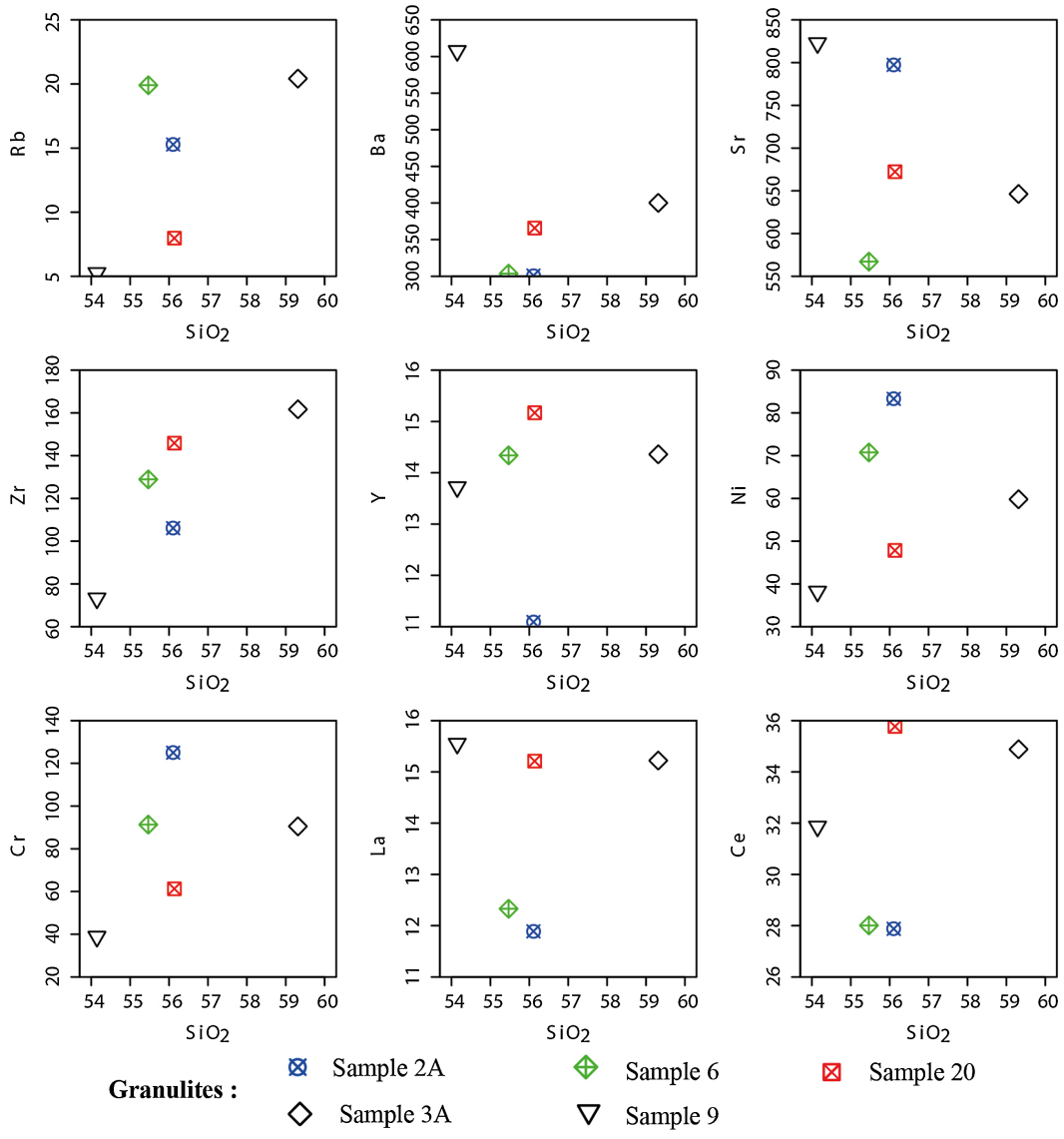

Figure 8. Traces elements vs. SiO_2 diagram [43] for rocks from the Anié unit.

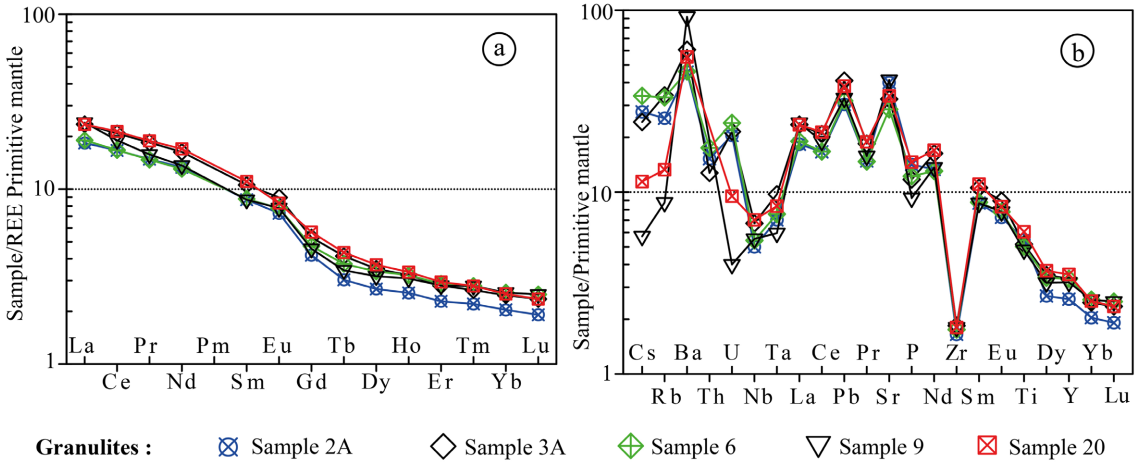

Figure 9. Spectra of rare earth elements normalized relative to the primitive mantle. (a) [44]; (b) [45].

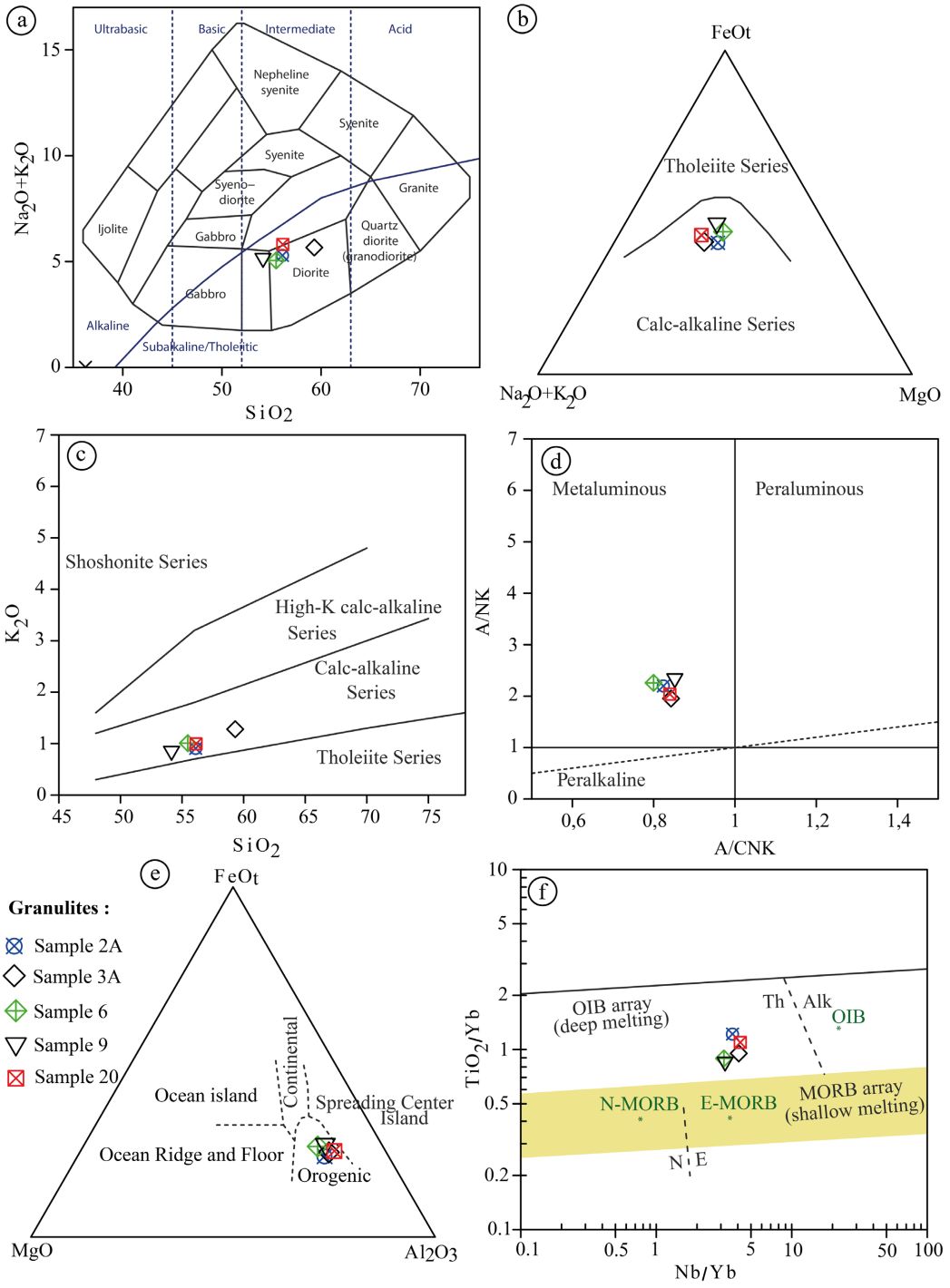

Figure 10. Geochemical classification plot showing the type (a), magmatic affinities (b, c, and d), and geotectonic context (e and f) of the Anié unit. (a): $Na_2O + K_2O$ vs SiO_2 [46]; (b): FeOt-($Na_2O + K_2O$)-MgO [47]; (c): SiO_2 vs K_2O [48]; (d): A/NK vs A/CNK [49]; (e): MgO-FeOt-Al_2O_3 [50]; (f): TiO_2/Yb-Nb/Yb [51].

by quartz-feldspar veins and veinlets. They are tectonically encased in gneiss. Deformation marks are characterized by submeridian NNW-SSE to NE-SW planar Sn + 1 structures with moderate to low dips towards the east. The linear Ln + 1 structures generally dip towards the NE and the brittle structures are oriented

WNW-ESE and N-S. The gneisses of the host rock show fractures oriented NW-SE and NNE-SSW. These major directions of brittle and semi-ductile deformation structures are coplanar with those of the Sn + 1 schistosity. The subhorizontal direction of the NE-dipping lineations observed in the Anié unit indicates dextral strike-slip movements associated with the ENE-WSW strike-slip zones [13] [19]. The WNW-ESE orientation of the fractures is consistent with that of the Pan-African fractures, with those oriented N-S being the most recent, in accordance with the data provided by [1]. The strike-slip movements and submeridian orientation of the veins are characteristics of the Kandi shear zone, of which the Anié unit represents the southern extension [40] [41]. The microstructures observed define three phases of deformation: a Dn phase (first phase of major tectonic deformation corresponding to the collision phase) highlighted by granulitization, a Dn + 1 phase (deformation phase following the Dn phase and corresponding to the tangential phase) corresponding to the main Sn + 1 foliation and associated with amphibolitization, and a Dn + 2 phase (deformation phase following phase Dn + 1 and corresponding to post-nappe folding) manifested by the folding of the main foliation [9] [10] [19] [40] [42].

Petrographic studies of the Anié inselbergs show that they are mainly composed of granulites. These are whitish to grayish granulites with a foliated structure and coarse foliation, and medium to fine grains. They are composed of plagioclase, prismatic amphibole, biotite, pyroxene, and quartz. They contain mesocratic basic enclaves. The different mineralogical associations of the samples described show the different metamorphic episodes that have affected these rocks. These granulites are characterized by the absence of garnet. This absence of garnet can be explained by the abundance of plagioclases in these granulites and the low-pressure conditions in which they were formed [2] [10] [11]. Amphibolization initiated the transformation of garnet-free granulites into amphibolites characterized by amphibole, plagioclase, and quartz paragenesis, indicating the transition from granulite to amphibolite facies [2] [4] [9] [10]. The surrounding gneisses are grayish, with a foliated structure, sometimes augen, and a granoblastic texture composed of feldspar, quartz, biotite, muscovite, and amphibole.

The geochemical study of the Anié unit shows that the rocks in this unit are metaluminous and have calc-alkaline affinities. They are mainly granulites. The richness of these rocks in TiO_2 and P_2O_5 is consistent with the appearance of titanium and apatite in these rocks, respectively [27] [52]. The depletion in Al_2O_3 and CaO suggests fractional crystallization of pyroxenes and calcic plagioclases in these rocks. Their poverty in FeOt and MgO indicates fractional crystallization of ferromagnesian minerals (pyroxene and amphibole) in these rocks [10] [53]. Negative anomalies in Nb-Ta and Zr indicate the influence of crustal material recycling. The good linear correlation in [9] diagrams reflects the role of fractional crystallization in the differenciation process during the evolution of the parent magmas of the rocks in this unit. The negative anomalies in Nb-Ta and Zr observed in the granulites of the Anié unit are characteristic of calc-alkaline magmas

in subduction zones [10] [11] [52]. The sloping aspect of the rare earth spectra is marked by low HREE fractionation and is thought to be associated with subduction. Geotectonic discrimination diagrams indicate that these rocks are calc-alkaline and derive from an OIB (oceanic island basalts) type mantle source that was subsequently modified in a subduction context [11] [27] [54]. This subduction resulted from submeridian thrusting that contributed to the formation of the Pan-African Dahomeyide belt [13].

It should be noted that the geochemical conclusions of this study are based on a limited number of samples (n = 5). Therefore, the proposed interpretations should be considered preliminary, calling for further research on a more extensive data set in order to better constrain the geological evolution of the Anié unit studied.

6. Conclusions

The lithostructural study of the Anié inselbergs revealed planar and linear structures expressing phases Dn, Dn + 1, and Dn + 2 of Pan-African tangential tectonics. The granulites of these inselbergs are tectonically encased in gneiss.

Petrographic studies of these inselbergs have identified granulites with a mineralogy of plagioclase, clinopyroxene, amphibole, biotite, and quartz. This paragenesis shows that these rocks underwent metamorphism in the granulite facies with retrogression in the amphibolite facies. The Anié unit therefore underwent tectonic-metamorphic evolution ranging from granulitization to retrograde metamorphism in the amphibolite facies.

Geochemical characterization shows that the rocks of the Anié unit are metaluminous and calc-alkaline. Inter-element variations indicate that these rocks evolved from a fractional crystallization process accompanied by crustal contamination. They were formed in an orogenic context. They are crustal basement rocks uplifted by Pan-African tectonics into crustal complexes. Geochemical trends clearly indicate their emplacement in a subduction context.

The rocks of the Anié unit show enrichment in LREE relative to HREE and subflat HREE spectra. Multi-element spectra show that most rocks are rich in mobile elements (Ba) and have negative anomalies in Nb-Ta and P. These characteristics are similar to those of rocks derived from an enriched mantle source and metasomatized during a subduction event.

Conflicts of Interest

The authors declare no conflicts of interest regarding the publication of this paper.

References

[1] Ménot, R.P. and Seddoh, K.F. (1980) Le massif basique stratifié précambrien de Djabatoure-Soutouboua (région centrale du Togo, Afrique de l'Ouest). Pétrologie et évolution métamorphique. *Bulletin du Bureau de recherches geologiques et minieres*, **4**, 319-337. https://www.researchgate.net/publication/260887781

[2] Agbossoumondé, Y. (1998) Les complexes ultrabasiques de la chaîne panafricaine au Togo (Axe Agou-Atakpamé, Sud-Togo). Etude pétrographique, minéralogique et

géochimique. Thèse, Jean Monnet University.

[3] Attoh, K. (1998) High-Pressure Granulite Facies Metamorphism in the Pan-African Dahomeyide Orogen, West Africa. *The Journal of Geology*, **106**, 236-246. https://doi.org/10.1086/516019

[4] Agbossoumonde, Y., Menot, R.P. and Guillot, S. (2001) Metamorphic Evolution of Neoproterozoic Eclogites from South Togo (West Africa). *Journal of African Earth Sciences*, **33**, 227-244. https://doi.org/10.1016/s0899-5362(01)80061-0

[5] Tairou, M.S. and Affaton, P. (2013) Structural Organization and Tectono-Metamorphic Evolution of the Pan-African Suture Zone: Case of the Kabye and Kpaza Massifs in the Dahomeyide Orogen in Northern Togo (West Africa). *International Journal of Geosciences*, **4**, 166-182. https://doi.org/10.4236/ijg.2013.41015

[6] Ménot, R.P. (1977) Les massifs basiques et ultrabasiques antémétamorphiques de la bordure Ouest du mole Dahoméo-Nigérian. https://www.researchgate.net/publication/327822999

[7] Menot, R.P. (1980) Les massifs basiques et ultrabasiques de la zone mobile pan-Africaine au Ghana, Togo et Benin; Etat de la question. *Bulletin de la Société Géologique de France*, **7**, 297-303. https://doi.org/10.2113/gssgfbull.s7-xxii.3.297

[8] Ménot, R.P. (1982) Les éclogites des Monts Lato: Un témoin de l'évolution tectono-métamorphique de la chaîne pan-africaine du Togo (Afrique de l'Ouest). *Document du Laboratoire de Géologie de Lyon*, No. 87, 63 p. https://www.persee.fr/doc/geoly_0750-6635_1982_num_87_1_1513

[9] Sabi, B.E. (2007) Etude pétrologique et structurale du Massif Kabyè, Nord-Togo. Thèse Doctorat, University of Lomé.

[10] Kpanzou, S.A.M. (2023) Contribution à l'étude du complexe basique-ultrabasique de Djabatouré-Anié (Centre-Togo): Caractéristiques pétrostructurales, géochimiques et indices de minéralisations associés. Thèse de Doctorat unique, University of Lomé.

[11] Duclaux, G. (2003) Etude pétrologique et structurale des massifs basiques et ultrabasiques de la zone de suture panafricaine de la chaîne des Dahomeyides au Togo: Implications, géodynamiques. Université Jean Monnet.

[12] Sylvain, J.P., Collart, J., Aregba, A. and Godonou, S. (1986) Notice explicative de la carte géologique 1/500.0000è du Togo, Mém. No. 6, D.G.M.G./B.N.R.M., Lomé-Togo.

[13] Affaton, P. (1990) Le bassin des Volta (Afrique de l'Ouest): Une marge passive d'âge protérozoïque supérieur, tectonisée au Panafricain (600±50 Ma). https://horizon.documentation.ird.fr/exl-doc/pleins_textes/pleins_textes_2/etudes_theses/31718.pdf

[14] Caby, R. (1989) Precambrian Terranes of Benin-Nigeria and Northeast Brazil and the Late Proterozoic South Atlantic Fit. In: *Terranes in the Circum-Atlantic Paleozoic Orogens*, Geological Society of America, 145-158. https://doi.org/10.1130/spe230-p145

[15] Affaton, P., Gelard, J.P. and Simpara, N. (1991) Paléocontraintes enregistrées par la fracturation dans l'unité structurale de l'Atacora (Chaîne Panafricaine des Dahomeyides, Togo). *Comptes rendus de l'Académie des Sciences*, **312**, 763-768. https://pascal-francis.inist.fr/vibad/index.php?action=getRecordDetail&idt=19679359

[16] Attoh, K., Dallmeyer, R.D. and Affaton, P. (1997) Chronology of Nappe Assembly in the Pan-Africa Dahomeyide Orogen, West Africa: Evidence from $^{40}Ar/39^{Ar}$ Mineral Ages. *Precambrian Research*, **82**, 153-171. https://doi.org/10.1016/s0301-9268(96)00031-9

[17] Ganade de Araujo, C.E., Rubatto, D., Hermann, J., Cordani, U.G., Caby, R. and Basei, M.A.S. (2014) Ediacaran 2,500-km-Long Synchronous Deep Continental Subduction in the West Gondwana Orogen. *Nature Communications*, **5**, Article No. 5198. https://doi.org/10.1038/ncomms6198

[18] Simpara, N., Sougy, J. and Trompette, R. (1985) Lithostratigraphie et structure du Buem unité externe de la chaine panafricaine des Dahomeyides dans la region de Bassar (Togo). *Journal of African Earth Sciences* (1983), **3**, 479-486. https://doi.org/10.1016/s0899-5362(85)80091-9

[19] Tairou, M.S. (2006) La tectonique tangentielle panafricaine au Nord-Togo. Thèse Doctorat, University of Lomé.

[20] Simpara, N. (1978) Etude géologique et structurale des unités externes de la chaîne panafricaine (600 Ma) des Dahomeyides dans la région de Bassar (Togo). Thèse, Paul Cézanne University.

[21] Affaton, P., Sougy, J. and Trompette, R. (1980) The Tectono-Stratigraphic Relationships between the Upper Precambrian and Lower Paleozoic Volta Basin and the Pan-African Dahomeyide Orogenic Belt (West Africa). *American Journal of Science*, **280**, 224-248. https://doi.org/10.2475/ajs.280.3.224

[22] Agbossoumondé, Y., Ménot, R.P., Paquette, J.L., Guillot, S., Yéssoufou, S. and Perrache, C. (2007) Petrological and Geochronological Constraints on the Origin of the Palimé–amlamé Granitoids (South Togo, West Africa): A Segment of the West African Craton Paleoproterozoic Margin Reactivated during the Pan-African Collision. *Gondwana Research*, **12**, 476-488. https://doi.org/10.1016/j.gr.2007.01.004

[23] Tairou, M.S., Affaton, P. and Sabi, B.E. (2009) Tectono-Metamorphic Evolution of the Mo and Kara-Niamtougou Orthogneic Suites, Northern Togo. *Global Journal of Geological Sciences*, **7**, 93-100. https://www.researchgate.net/publication/287411921

[24] Caen-Vachette, M., Pinto, K.J.M. and Roques, M. (1979) Plutons éburnéens et métamorphisme dans le socle cristallin de la chaîne panafricaine au Togo et au Bénin. *Revue de Geographie Physique et de Geologie Dynamique*, **21**, 351.

[25] Kalsbeek, F., Affaton, P., Ekwueme, B., Frei, R. and Thrane, K. (2012) Geochronology of Granitoid and Metasedimentary Rocks from Togo and Benin, West Africa: Comparisons with NE Brazil. *Precambrian Research*, **196**, 218-233. https://doi.org/10.1016/j.precamres.2011.12.006

[26] Aidoo, F., Sub, F.Y., Liang, T. and Nude, P.M. (2020) New insight into the Dahomeyide Belt of Southeastern Ghana, West Africa: Evidence of Arc-Continental Collision and Neoarchaean Crustal Reworking. *Precambrian Research*, **347**, Article 105836. https://doi.org/10.1016/j.precamres.2020.105836

[27] Tairou, M.S., Miningou, Y.M.W., Da Costa, Y.D. and Kwekam, M. (2022) Petrostructural and Geochemical Characteristics of the Metamagmatites in the External Zone of the Dahomeyides Belt: Case of the Kantè Serpentinites (Northern Togo). *International Journal of Geosciences*, **13**, 779-792. https://doi.org/10.4236/ijg.2022.139039

[28] Kwayisi, D., Amponsah, P.O., Agra, N.A., Nunoo, S., Thompson, J., Kazapoe, R.W., *et al.* (2024) Neoproterozoic Passive Margin Formation and Evolution during the Rodinia-gondwana Supercontinent Cycle at the Eastern Margin of the West African Craton. *Geological Magazine*, **161**, 1-23. https://doi.org/10.1017/s001675682400027x

[29] Attoh, K. and Nude, P.M. (2008) Tectonic Significance of Carbonatites and Ultrahigh-Pressure Rocks in the Pan-African Dahomeyide Suture Zone, Southeastern Ghana. In: Ennih, N. and Liégeois, J.P., *The Boundaries of the West African Craton*, Special Publications, 217-231.

[30] Affaton, P., Kröner, A. and Seddoh, K.F. (2000) Pan-African Granulite Formation in

the Kabye Massif of Northern Togo (West Africa): Pb-Pb Zircon Ages. *International Journal of Earth Sciences*, **88**, 778-790. https://doi.org/10.1007/s005310050305

[31] Agbossoumondé, Y., Guillot, S. and Ménot, R.P. (2004) Pan-African Subduction-Collision Event Evidenced by High-P Coronas in Metanorites from the Agou Massif (Southern Togo). *Precambrian Research*, **135**, 1-21. https://doi.org/10.1016/j.precamres.2004.06.005

[32] Attoh, K. and Morgan, J. (2004) Geochemistry of High-Pressure Granulites from the Pan-African Dahomeyide Orogen, West Africa: Constraints on the Origin and Composition of the Lower Crust. *Journal of African Earth Sciences*, **39**, 201-208. https://doi.org/10.1016/j.jafrearsci.2004.07.048

[33] Duclaux, G., Ménot, R.P., Guillot, S., Agbossoumondé, Y. and Hilaret, N. (2006) The Mafic Complex of the Kabyé Massif (North Togo and North Benin): Evidence of a Pan-African Granulitic Continental Arc Root. *Precambrian Research*, **151**, 101-118.

[34] Attoh, K., Corfu, F. and Nude, M.P. (2007) U-Pb Zircon Age of Deformed Carbonatite and Alkaline Rocks in the Pan-African Dahomeyide Suture Zone, West Africa. *Precambrian Research*, **155**, 251-260.

[35] Kwayisi, D., Elburg, M. and Lehmann, J.P. (2022) Preserved Ancient Oceanic Lithosphere within the Buem Structural Unit at the Eastern Margin of the West African Craton. *Lithos*, **410**, Article 106585. https://doi.org/10.1016/j.lithos.2021.106585

[36] Abdelsalam, M.G., Liégeois, J. and Stern, R.J. (2002) The Saharan Metacraton. *Journal of African Earth Sciences*, **34**, 119-136. https://doi.org/10.1016/s0899-5362(02)00013-1

[37] Caen-Vachette, M. (1975) Age Pan-Africain des granites de Sinendé, Save et Fita (Dahomey). *Comptes rendus de l'Académie des Sciences*, 1793-1795.

[38] Rahaman, M.A., Ukpong, E.E. and Azmatullah, M. (1988) Geology of Parts of the Oban Massif, Southeastern Nigeria. *Journal of Geology & Mining*, **15**, 38-56.

[39] Caby, R. and Boessé, J.M. (2001) Pan-African Nappe System in Southwest Nigeria: The Ife-Ilesha Schist Belt. *Journal of African Earth Sciences*, **33**, 211-225. https://doi.org/10.1016/s0899-5362(01)80060-9

[40] Adissin, G.L. (2012) La zone de cisaillement de Kandi et le magmatisme associé dans la région de Savalou-Dassa (Bénin): Étude structurale, pétrologique et géochronologique. Thèse de Doctorat unique des Universités Jean Monnet Saint-Etienne et d'Abomey-Calavi, 276 p.

[41] Alayi, G. (2018) Les granitoïdes tardifs de la chaîne panafricaine des Dahomeyides au Togo: Étude pétro-structurale, géochimique et géochronologique. Thèse Doctorat, FDS, University of Lome, 256 p.

[42] Alayi, G., Kpanzou, S.A.M., Agbossoumondé, Y., Padaro, E., Menot, R. and Tairou, M.S. (2023) Petrology, Age and Geodynamic Implication of the Panafrican Granitoids Associated with the Glito-Kpatala Shear Zone (South-East Togo). *International Journal of Geosciences*, **14**, 1193-1225. https://doi.org/10.4236/ijg.2023.1412061

[43] Harker, A. (1909) The Natural History of Igneous Rocks. Methuen and Co.

[44] Nakamura, N. (1974) Determination of REE, Ba, Fe, Mg, Na and K in Carbonaceous and Ordinary Chondrites. *Geochimica et Cosmochimica Acta*, **38**, 757-775. https://doi.org/10.1016/0016-7037(74)90149-5

[45] McDonough, W.F. and Sun, S.S. (1995) The Composition of the Earth. *Chemical Geology*, **120**, 223-253. https://doi.org/10.1016/0009-2541(94)00140-4

[46] Cox, K.G., Bell, J.D. and Pankhurst, R.J. (1979) The Interpretation of Igneous Rocks. George Allen & Unwin, 450 p.

[47] Irvine, T.N. and Baragar, W.R.A. (1971) A Guide to the Chemical Classification of the Common Volcanic Rocks. *Canadian Journal of Earth Sciences*, **8**, 523-548. https://doi.org/10.1139/e71-055

[48] Peccerillo, A. and Taylor, S.R. (1976) Geochemistry of Eocene Calc-Alkaline Volcanic Rocks from the Kastamonu Area, Northern Turkey. *Contributions to Mineralogy and Petrology*, **58**, 63-81. https://doi.org/10.1007/bf00384745

[49] Shand, S.J. (1943) Eruptive Rocks. Their Genesis, Composition, Classification and Their Relations to Ore Deposits. 2nd Edition, Murby London, 444 p. https://www.scirp.org/(S(czeh2tfqyw2orz553k1w0r45))/reference/ReferencesPapers.aspx?ReferenceID=1945539

[50] Pearce, J.A. and Gale, G.H. (1977) Identification of Ore-Deposition Environment from Trace-Element Geochemistry of Associated Igneous Host Rocks. *Geological Society*, *London*, *Special Publications*, **7**, 14-24. https://doi.org/10.1144/gsl.sp.1977.007.01.03

[51] Pearce, J.A. (2008) Geochemical Fingerprinting of Oceanic Basalts with Applications to Ophiolite Classification and the Search for Archean Oceanic Crust. *Lithos*, **100**, 14-48. https://doi.org/10.1016/j.lithos.2007.06.016

[52] Guillot, S., Agbossoumondé, Y., Bascou, J., Berger, J., Duclaux, G., Hilairet, N., *et al.* (2019) Transition from Subduction to Collision Recorded in the Pan-African Arc Complexes (Mali to Ghana). *Precambrian Research*, **320**, 261-280. https://doi.org/10.1016/j.precamres.2018.11.007

[53] Hamlaoui, H., Laouar, R., Bouhlel, S. and Boyce, A.J. (2020) Caractéristiques pétrologiques et géochimiques des roches magmatiques d'El Aouana, NE algérien. *Estudios Geológicos*, **76**, e124. https://doi.org/10.3989/egeol.43391.510

[54] Kpanzou, S.A.M., Kassegne, K.E., Alayi, G., Padaro, E., Togbe, K.A., Tairou, M.S., *et al.* (2025) Petrology and Mining Potential of the Niki-Niki Basic to Ultrabasic Massif in Togo, West Africa. *Journal of Geoscience and Environment Protection*, **13**, 97-117. https://doi.org/10.4236/gep.2025.136008